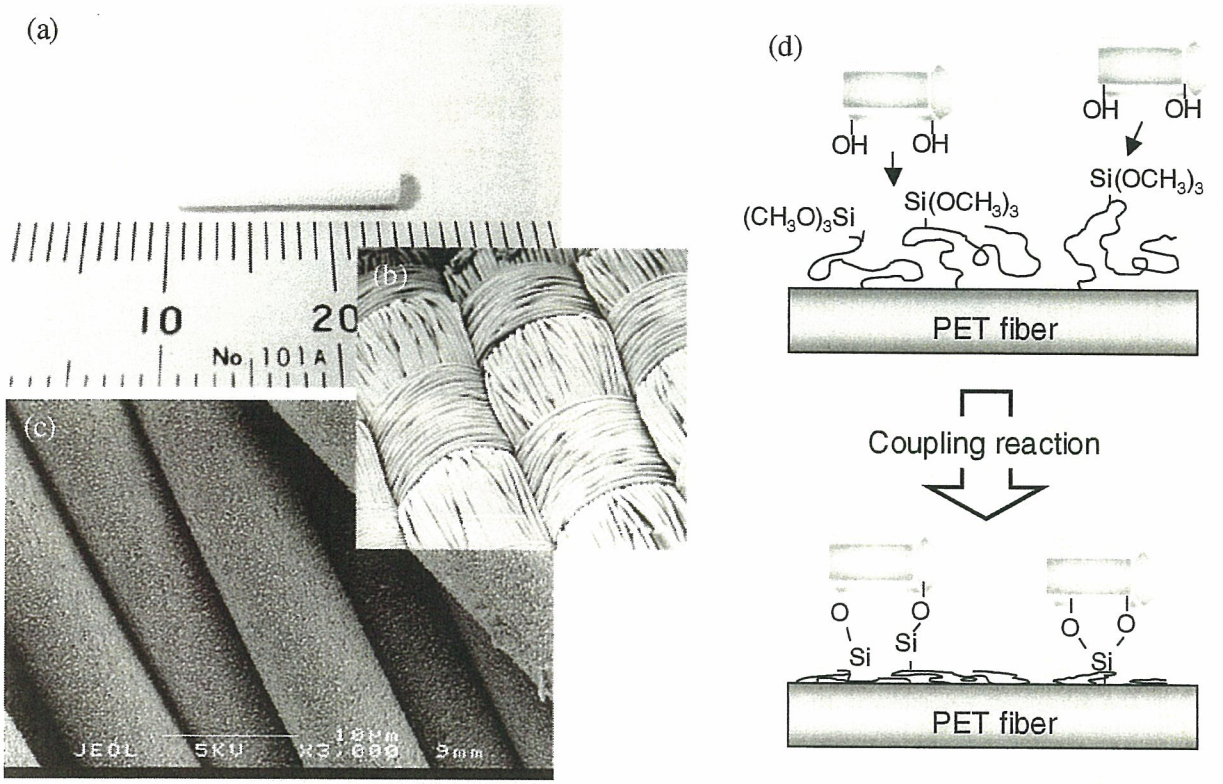

Figure 25. The images show prototype of an artificial blood vessel made of HAp/PET composite. (a) External view of the prototype. (b, c) Lower and higher magnification of SEM images of HAp/PET fibers of inside of the prototype. (d) Schematic presentation of the reaction process of calcined HAp nanoparticles covalently coated on a PET fiber.

observed by a fluorescence microscope. It was found that the number of cells adhered on HAp/PET was qualitatively the same as that of collagen-coated PET, although the cells seldom adhered on the original PET for such a short period of incubation. This phenomenon can be explained because cell adhesion proteins such as fibronectin or vitronectin in a culture medium may be favorably adsorbed on the HAp surface [22]. In other words, calcined HAp coating on popular biomedical substrates is effective to obtain the affinity of cells without using biological scaffold proteins such as collagen or gelatin. The HAp/PET composite is very meaningful for biological safety in medical fields today when the danger of BSE infection by using proteins derived from a bovine animal is trumpeted loudly. A prototype of artificial blood vessel made of the HAp/PET composite was fabricated (Fig. 25). The calcined HAp nanoparticles were thoroughly coated on PET fibers of inside and outside of an artificial blood vessel. The effect of HAp nanocrystals on it through animal implantation experiments *in vivo* are under evaluation.

5. CONCLUSIONS

Well-crystallized and calcined HAp nanoparticles with free impurities were synthesized through the modified emulsion process. The morphology and size of the HAp nanoparticles were drastically changed by altering the reaction temperature. Calcined HAp nanoparticles with spherical, or rodlike, morphologies well-dispersed in a liquid media were also successfully prepared by calcinations using an antisintering agent interspersed between or surrounding the particles, followed by removal of the agent. The inorganic-organic composite, consisting of calcined HAp nanoparticles and polymer substrates, were prepared through chemical bonding, such as covalent or ionic bonding. The elasticity of the composite was not change compared with the original polymer substrates. The cell-adhesion test shows that the HAp/polymer substrate improves bioactivity compared with original substrates. Cells were also able to penetrate into the gaps between the inorganic-organic composite in a three-dimensional tangle. A percutaneous device and an artificial blood vessel were fabricated from the HAp composite polymer fibers have been examined by animal implant experiments.

Preparation of composites consisting of calcined HAp nanoparticles and polymer substrates, for examples, mixture, *in situ* or nanochemical bonding methods, is necessary for nanoscaled observation from the points of view of the bulk structures, surface properties, and biological interactions. For our composite, especially, the size, coverage ratio, or strength of chemical bonding of sintered HAp nanoparticles are assumed to be important for interactions with biomolecules such as proteins, cells, and tissues to develop medical devices. This composite material is expected to

establish a novel concept for fabrication of an inorganic-organic composite as biocompatible materials for hard and soft tissue.

ACKNOWLEDGMENTS

The authors are grateful to Dr. Junzo Tanaka, Biomaterials Center, National Institute for Materials Science, and Prof. Akio Kisida, Institute of Biomaterials and Bioengineering, Tokyo Medical and Dental University, for their helpful advices and supports. A series of the study about the development of the nanocomposite was financially supported in part by research programs of Japan Science and Technology Corporation (JST)—CREST, PRESTO, and Innovation Plaza Osaka—and promoting projects on Comprehensive Research on Cardiovascular Diseases.

REFERENCES

1. H. Aoki, "Medical Applications of Hydroxyapatite." Ishiyaku, EuroAmerica, Tokyo, 1994.
2. V. Midy, C. Rey, E. Bres, and M. Dard, *J. Biomed. Mater. Res.* 41, 405 (1998).
3. C. C. Veheyen, J. R. de Wijn, C. A. van Blitterswijk, K. de Groot, and P. M. Rozing, *J. Biomed. Mater. Res.* 27, 433 (1993).
4. M. Wang, R. Joseph, and W. Bonfield, *Biomaterials* 19, 2357 (1998).
5. S. I. Stupp and G. W. Ciegler, *J. Biomed. Mater. Res.* 26, 169 (1992).
6. K. Kato, Y. Eika, and Y. Ikada, *J. Biomed. Mater. Res.* 32, 687 (1996).
7. M. Kikuchi, S. Itoh, S. Ichinose, K. Shinomiya, and J. Tanaka, *Biomaterials* 22, 1705 (2001).
8. M. C. Chang, T. Ikoma, M. Kikuchi, and J. Tanaka, *J. Mater. Sci. Mater. Med.* 13, 993 (2002).
9. S. Ito, M. Kikuchi, Y. Koyama, K. Takakuda, K. Shinomiya, and J. Tanaka, *Cell Transplant.* 13, 451 (2004).
10. H. M. Kim, T. Himeno, T. Kokubo, and T. Nakamura, *Biomaterials* 26, 4366 (2005).
11. G. J. Liu, F. Miyaji, T. Kokubo, H. Takadama, T. Nakamura, and A. Murakami, *J. Mater. Sci. Mater. Med.* 9, 61 (1998).
12. T. Taguchi, A. Kishida, and M. Akashi, *Chem. Lett.* 711 (1998).
13. T. Furuzono, T. Taguchi, A. Kishida, M. Akashi, and Y. Tamada, *J. Biomed. Mater. Res.* 50, 344 (2000).
14. T. Taguchi, Y. Muraoka, H. Matsuyama, A. Kishida, and M. Akashi, *Biomaterials* 22, 53 (2001).
15. K. de Groot, R. Geesink, C. P. A. T. Klein, and P. Serekian, *J. Biomed. Mater. Res.* 21, 1375 (1987).
16. T. Furuzono, D. Walsh, K. Sato, K. Sonoda, and J. Tanaka, *J. Mater. Sci. Lett.* 20, 111 (2001).
17. K. Sonoda, T. Furuzono, D. Walsh, K. Sato, and J. Tanaka, *Solid State Ionics* 151, 321 (2002).
18. T. Furuzono, A. Kishida, and J. Tanaka, *J. Mater. Sci. Mater. Med.* 15, 19 (2004).
19. A. Korematsu, T. Furuzono, S. Yasuda, J. Tanaka, and A. Kishida, *J. Mater. Sci.* 39, 3221 (2004).
20. A. Korematsu, T. Furuzono, S. Yasuda, J. Tanaka, and A. Kishida, *J. Mater. Sci. Mater. Med.* 16, 67 (2005).
21. T. Furuzono, S. Yasuda, T. Kimura, Si. Kyotani, J. Tanaka, and A. Kishida, *J. Artif. Organs* 7, 137 (2004).
22. T. Furuzno, M. Masuda, M. Okada, S. Yasuda, H. Kadono, R. Tanaka, and K. Miyatake, *ASAIO J.* 7, 137 (2004).
23. M. Taniguchi, H. Takeyama, I. Mizuno, N. Shinagawa, J. Yura, N. Yoshiyama, and H. Aoki, *Jpn. J. Artif. Organs* 20, 460 (1991).
24. P. M. Zabetakis, C. M. Cotell, D. B. Chrisery, and R. C. Auyeung, *ASAIO J.* 40, M896 (1994).
25. T. Furuzono, K. Sonoda, and J. Tanaka, *J. Biomed. Mater. Res.* 56, 9 (2001).
26. T. Furusono, P. Wang, A. Korematsu, K. Miyazaki, M. Oido-Mori, Y. Kowashi, K. Ohura, J. Tanaka, and A. Kishida, *J. Biomed. Mater. Res. B: Appl. Biomater.* 65B, 217 (2003).
27. M. Jarcho, C. H. Bolen, M. B. Thomas, J. Bobick, J. F. Kay, and R. H. Doremus, *J. Mater. Sci.* 11, 2027 (1976).
28. H. K. Schmidt, *Mol. Cryst. Liq. Cryst.* 353, 165 (2000).
29. B. L. Cushing, V. L. Kolesnichenko, and C. J. O'Connor, *Chem. Rev.* 104, 3893 (2004).
30. S. Somiya, K. Ioku, and M. Yoshimura, *Mater. Sci. Forum* 34–36, 371 (1988).
31. M. Yoshimura, H. Suda, K. Okamoto, and K. Ioku, *J. Mater. Sci.* 29, 3399 (1994).
32. A. D. Papargyris, A. I. Botis, and S. A. Papargyri, *Key Eng. Mater.* 206–213, 83 (2002).
33. Y. Masuda, K. Matsubara, and S. Sakka, *J. Ceram. Sci. Jpn.* 98, 1226 (1990).
34. C. Sanchez and J. Livage, *New J. Chem.* 14, 513 (1990).
35. H. K. Schmidt, E. Geiter, M. Mennig, H. Krug, C. Becker, and R. P. Winkler, *J. Sol.-Gel Sci. Tech.* 13, 397 (1998).
36. G. K. Lim, J. Wang, and S. C. Ng, L. M. Gan, *Mater. Lett.* 28, 431 (1996).
37. G. Guo, Y. Sun, Z. Wang, and H. Guo, *Ceram. Int.* 31, 869 (2005).
38. Y. Wu and S. Bose, *Langmuir* 21, 3232 (2005).
39. G. K. Lim, J. Wang, S. C. Ng, and L. M. Gan, *Mater. Lett.* 28, 431 (1996).
40. W. H. Emerson and E. E. Fisher, *Arch. Oral Biol.* 7, 671 (1962).
41. R. Z. LeGeros, in "Calcium Phosphate in Oral biology and Medicine" (H. M. Hyers, Ed.). Karger, New York, 1991.
42. L. Qi, J. Ma, M. Cheng, and Z. Zhao, *J. Mater. Sci. Lett.* 16, 1779 (1997).
43. G. K. Lim, J. Wang, S. C. Ng, and L. M. Gan, *J. Mater. Chem.* 9, 1635 (1999).
44. S. Mann, J. Didymus, N. P. Sanderson, B. R. Heywood, and E. J. A. Samper, *J. Chem. Soc. Faraday Trans.* 86, 1873 (1990).
45. J. Frenkel, *J. Phys. USSR* 9, 385 (1945).
46. G. C. Kuczynski, *Trans. AIME* 185, 169 (1949).
47. J. E. Barralet, S. M. Best, and W. Bonfield, *J. Mat. Sci. Mater. Med.* 11, 719 (2000).
48. E. Landi, A. Tampieri, G. Celotti, and S. Sprio, *J. Eur. Ceram. Soc.* 20, 2377 (2000).
49. D. Bernache-Assollant, A. Ababoua, E. Championa, and M. Heughebaertb, *J. Eur. Ceram. Soc.* 23, 229 (2003).
50. J. E. Carless and A. A. Foster, *J. Pharmaceut. Pharmacol.* 18, 697 (1966).
51. M. Wei, A. J. Ruys, B. K. Milthorpe, and C. C. Sorrell, *J. Biomed. Mater. Res.* 45, 11 (1999).
52. K. Nishizawa, M. Toriyama, T. Suzuki, Y. Kawamoto, Y. Yokogawa, and F. Nishizawa, *Chem. Soc. Jpn.* 1, 63 (1995).
53. R. Labella, M. Braden, and S. Deb, *Biomaterials* 15, 1197 (1994).
54. A. M. P. Dupraz, J. R. de Wijn, S. A. T. vd de Meer, and K. de Groot, *J. Biomed. Mater. Res.* 30, 231 (1996).
55. Q. Kiu, J. R. de Wijn, K. de Groot, and C. A. van Blitterswijk, *Biomaterials* 19, 1067 (1998).
56. P. E. Cranley, *Polym. Sci. Technol.* 29, 765 (1984).
57. T. Furuzono, K. Ishihara, N. Nakabayashi, and Y. Tamada, *J. Appl. Polym. Sci.* 73, 2541 (1999).
58. Q. Liu, J. R. de Wijn, and C. A. van Blitterswijk, *J. Biomed. Mater. Res.* 40, 257 (1998).
59. T. Kawasaki, *J. Chromatogr.* 544, 147 (1991).
60. Y. Abe, M. Kiyomura, K. Nagata, and N. Nakabayashi, *J. Jpn. Dent. Mater.* 5, 310 (1986).

61. M. Kikuchi, Y. Suetsugu, J. Tanaka, S. Itoh, S. Ichinose, K. Shinomiya, Y. Hiraoka, Y. Mandai, and S. Nakatani, in "Bioceramics, Proceedings of the 12th International Symposium on Ceramics in Medicine" (H. Ohgushi, G. W. Hastings, and T. Yoshikawa, Eds.), Vol. 12, p. 393. World Scientific Publishing, Singapore, 1999.
62. J. Tanaka and M. Kikuchi, *Ceram. Jpn.* 34, 543 (1999).
63. Nippon-Sen'I-Kikai-Gakkai, eds., Sangyoyo-sen'I-sizai Handbook, Tokyo, 1979, p. 8.
64. N. Yui, Y. Suzuki, H. Mori, and N. Okano, in "Surface Science of Crystalline Polymers" (N. Yui and M. Terano, Eds.), p. 121, Kodansha Scientific, Tokyo, 1996.
65. T. Furuzono, M. Iwasaki, S. Yasuda, A. Korematsu, T. Yoshioka, S. Ito, and A. Kishida, *J. Mater. Sci. Lett.* 32, 1737 (2003).
66. P. Hamerli, T. Weigel, T. Groth, and D. Paul, *Biomaterials* 24, 3989 (2003).
67. S. P. Massia and J. A. Hubbell, *J. Biomed. Mater. Res.* 25, 223 (1991).

大動脈瘤・大動脈解離診療のコツと落とし穴

編集● 田林 晄一
栗林 幸夫

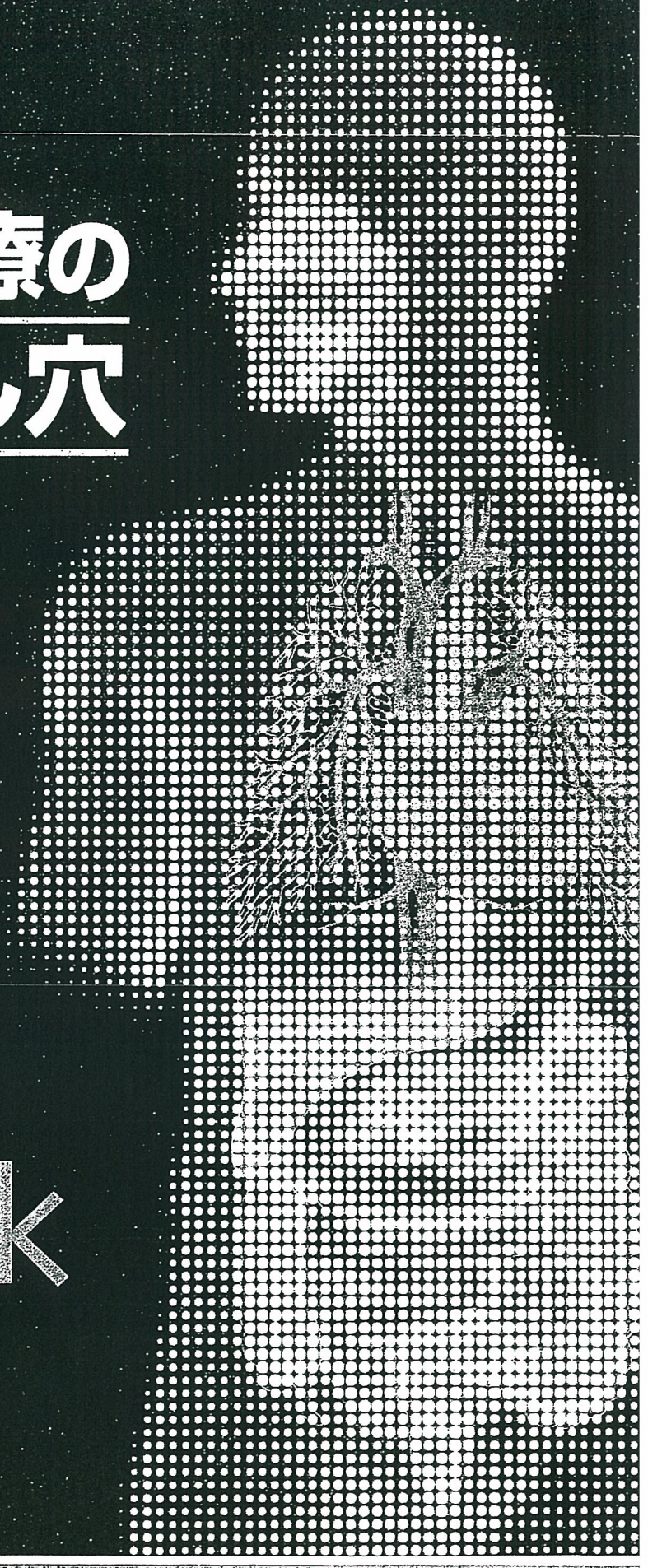

Pitfalls & Knack

中山書店

腹部大動脈瘤ステントグラフト治療において重要な側副血行のCT診断

田中 良一（国立循環器病センター）

ステントグラフトだけでは制御できない問題の一つにtype IIエンドリークがある

腹部大動脈瘤のステントグラフト治療は低侵襲性であることより，重症合併症を有する症例において有効な治療法だが，ステントグラフトだけでは制御できない問題の一つに主要分枝からの逆行性血流によるいわゆるtype IIエンドリークがある．また，瘤の形態によっては，内腸骨動脈など分枝の閉塞を必要とすることもあり，その分枝末梢に存在する組織への血流供給について検討しておくことも重要である．ここでは，CTにおいて判定できる側副血行のうち，腹部大動脈瘤ステントグラフト治療に関連すると思われるものを提示する．

大動脈関連の側副血行では腰動脈と下腸間膜動脈に注意

大動脈に関連した側副血行では，ステントグラフトtype IIエンドリークを起らす血管として腰動脈および下腸間膜動脈が重要である．ずれの血管も動脈硬化や瘤に関連する壁在血栓の影響で，前に閉塞していることもあるが，開存している場合はその，さや他の血管との末梢吻合に留意する必要がある．腰動脈，他のレベルの腰動脈や内腸骨動脈の分枝である腸腰動脈と吻合することがあり（❶），下腸間膜動脈は上腸間膜動脈と

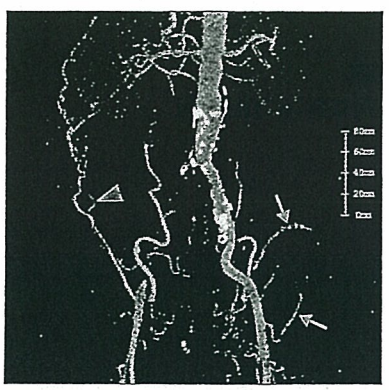

❶ 腰動脈・大腿動脈から内腸骨動脈分枝への吻合
造影CTアンギオグラフィ（最大値投影法）正面像．閉塞性動脈疾患により右総腸骨動脈および外腸骨動脈が閉塞．また，左内腸骨動脈も閉塞している．右では腰動脈から腸腰動脈への側副路（矢頭）が発達し，腰動脈から腸骨回旋動脈への側副路もみられる．左では内側および外側大腿回旋動脈から下殿動脈，上殿動脈への側副路（矢印）がみられる．また，本例では両側内胸動脈と吻合する下腹壁動脈も側副路として発達しているが，これらは下肢血流には関連するが，エンドリークに関与する側副路ではない．

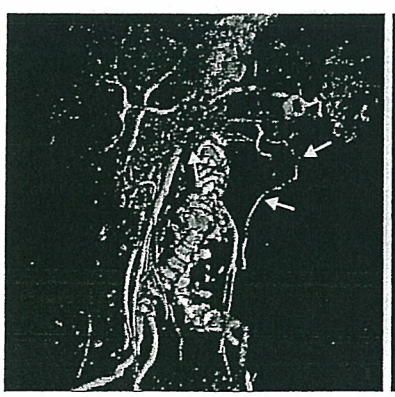

❷ 上腸間膜動脈から下腸間膜動脈への側副路
本例はステントグラフト留置後にエンドリークが残存した症例である．側副路をみやすいように大動脈の一部を削除している．上腸間膜動脈から下腸間膜動脈への側副路がみられる（矢印）．三次元再構成でわかりやすい術後の拡張した側副路を表示しているが，本例ではステントグラフト術前より横断像では上腸間膜動脈と下腸間膜動脈の連続がみられていた．

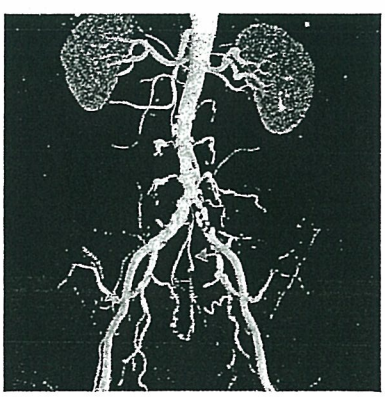

❸ 内腸骨動脈分枝どうしおよび正中仙骨動脈の吻合
左総腸骨動脈閉塞症例．右内腸骨動脈から左内腸骨動脈へ吻合がみられる．また，正中仙骨動脈も側副路として発達している（矢印）．

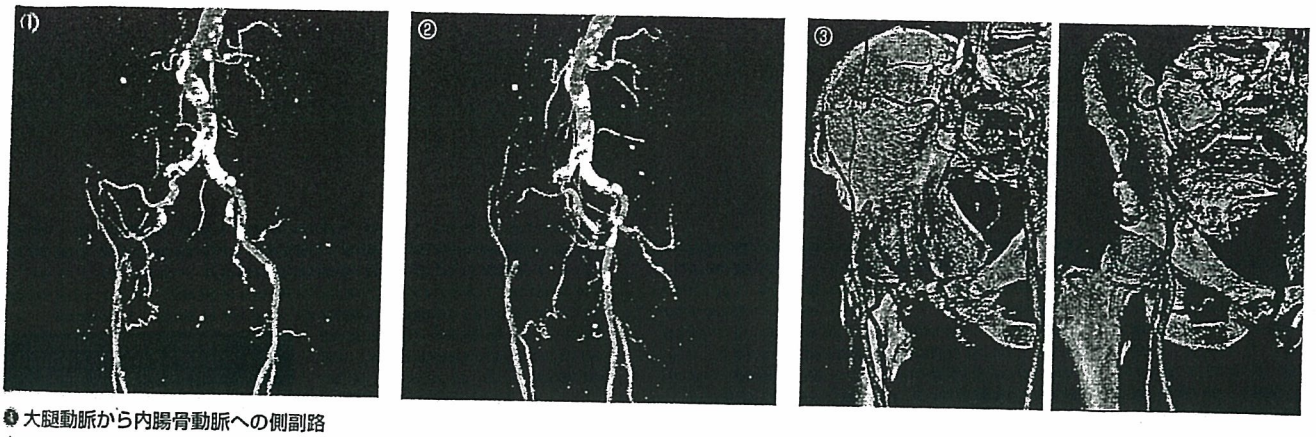

❶大腿動脈から内腸骨動脈への側副路
①正面像．右外腸骨動脈閉塞の症例の最大値投影法．内腸骨動脈から閉鎖動脈および外陰部動脈を介し，右総大腿動脈に連続する側副路を認める．本例では下肢への側副路として内腸骨動脈から大腿動脈方向へ血流があると考えられるが，内腸骨動脈閉塞の場合は逆流する側副路として重要である．
②左前斜位像．斜位にて側副路の連続が明瞭となっている．
③ボリュームレンダリング像．側副路と骨との関係がわかる．閉鎖孔を通る閉鎖動脈が拡張していることがわかる．

中結腸動脈を介して潜在的な側副路を形成する（❷）．これらは三次元画像では判定が難しい場合もあるが，二次元画像をたんねんに追跡すると連続性の有無を確認できる．開存している血管であるにもかかわらず，術前にこれらの側副血行となる血管との連続性を確認できる場合は，術後のエンドリーク発生に特に注意すべきであろう．また，正中仙骨動脈は内腸骨動脈の分枝である外側仙骨動脈と吻合することがある（❸）．

腸骨動脈関連の側副血行では治療前の側副路評価が重要

ステントグラフト治療の際，瘤の形態によっては内腸骨動脈の塞栓を行う必要がある．経験的に内腸骨動脈へは豊富な側副血行があることは認識されており，塞栓が問題となることは必ずしも多くない．しかし，瘤に伴って閉塞性動脈疾患を合併し塞栓すべき内腸骨動脈と反対側の内腸骨動脈に高度の狭窄や閉塞が存在する場合，腸管虚血の合併症を考慮しなくてはならず治療前の側副路評価は重要となる．通常，内腸骨動脈およびその分枝へは対側の内腸骨動脈分枝である外側仙骨動脈，子宮動脈，中直腸動脈，下膀胱動脈，閉鎖動脈内陰部動脈が吻合し連続する（❸）が，そのほかに腰動脈，正中仙骨動脈が側副路として有名である．ただし，これらの動脈は上記のようなステントグラフト留置の場合には有効な側副路としては機能しないことがあり，その場合は外陰部動脈から閉鎖動脈そして内腸骨動脈へ連続する側副路の発達は重要である（❹）．また，肋間動脈や肋下動脈からの側副路が吻合することもあり，これらの連続性を確認しておく必要がある．さらに，内側および外側大腿回旋動脈から下殿動脈，上殿動脈への側副路も評価が必要である．これらの評価においても三次元画像は必ずしも適当ではなく二次元画像をたんねんに追跡することが重要だが，十分に発達した側副路は丁寧に作成された三次元画像で評価が可能な場合もある（❶）．

2006年10月31日発行

臨床放射線 51巻11号（10月臨時増刊号）

Interventional Radiologyのコツ

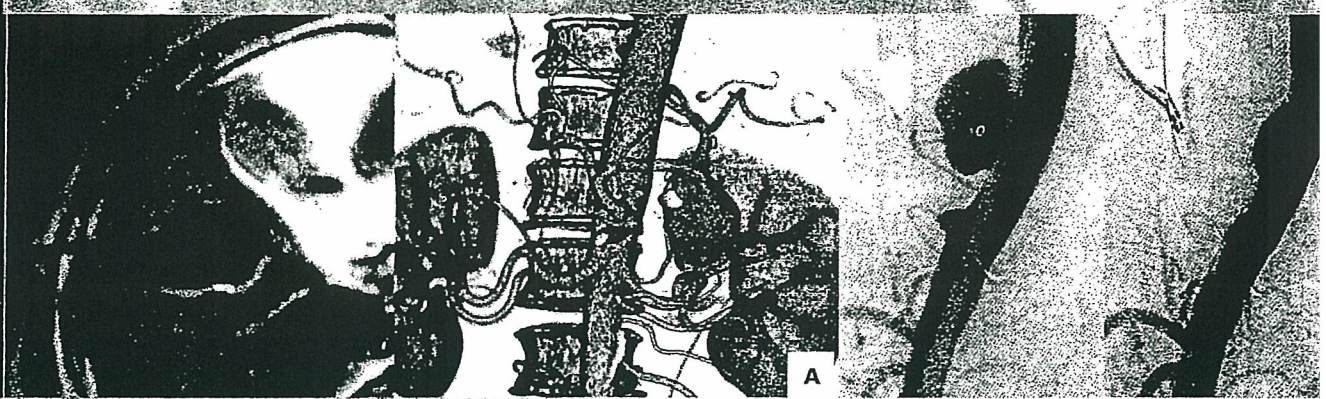

●編集 臨床放射線編集委員会

金原出版株式会社

骨盤下肢動脈の PTA/ステント

田中良一*

はじめに

骨盤から下肢動脈における閉塞性動脈疾患に対するPTAおよびステントはデバイスの発達とともに適応が広がり，一般的な治療法として行われるようになってきている。一方で，血管を詰める操作ではなく，広げて血流を確保する操作である点が一般的なinterventional radiology（IVR）とは異なる点であり，治療戦略の立て方も異なってくる。本稿では骨盤下肢動脈のPTAとステントについて領域ごとの治療成績の違いから，治療戦略の立て方およびデバイス選択や治療時のコツについて述べる。

❶ 骨盤下肢動脈における IVR の成績

末梢血管の閉塞性動脈疾患においてはTrans Atlantic Inter-Society Consensus（TASC）によるconsensus paperが2000年に出されており[1]，この内容はインターネットでも確認できる，(URL：www.tasc-pad.org)。これは1999年までのデータをまとめたものであり，現時点ではやや内容が古くなっているが，閉塞性動脈疾患における標準的な教科書であるといってもよいと思われる。(内容をアップデートしたEssential TASCでは2000年以降のデータを踏まえ，IVRの適応もやや拡大される様子である。)

腸骨動脈領域においては，ステント（図1）を用いることにより良好な成績を示すことが示されており[2-4]，TASC C，Dのような長区域病変であっても治療成績が良好であることが示されている[5]。一方で，大腿動脈においては様々な工夫がなされている[6-9]が，腸骨動脈と比較して治療成績は必ずしも満足いくものとはいえない。また，同領域におけるステント挿入は現在のところ明確な治療成績の改善をもたらすものではなく，また，大腿動脈の可動性に基づく遠隔期におけるステント破損の問題があり，ステント破損に伴う再狭窄のみならず，低い発生頻度ではあるようだが血管損傷による仮性動脈瘤形成などの問題点もある。この領域においては，Boliaら[10][11]によってsubintimal angioplastyが提唱されてから，長区域閉塞に対する血管形成術が盛んに行われるようになった歴史があるが，原法はステントを使用せずに開存を得るための方法であった。しかし，昨今，ステントが多用されるようになり，十分な拡張が行われないままステントが使用されていることは憂慮すべきであろう。

下腿においては重症虚血趾に対する治療が主となる[12-16]が，非常に状態が悪い血管に対して治療を行うこととなり，閉塞病変に対する治療が必要となる事も多い。治療が不成功の場合，趾切断に至るリスクも十分にあることを念頭におく必要がある。

❷ 部位別の治療の特徴とコツ

1）腸骨動脈

腸骨動脈は国際的にもIVR治療のコンセンサスが得られている領域であり，ステントを含めデバイスの選択枝も最も多い領域である。以前は血管造影ですべて判断せざるを得なかったが，現在では超音波検査，MRI，CTと様々なモダリ

* 岩手医科大学放射線科
〔索引用語：PTA，ステント，下肢動脈〕

ティを駆使して事前に情報を収集できる。まず，治療対象となる病変の局在と性状を把握することが大切で，病変の石灰化の有無，病変部および前後の血管におけるremodelingの有無が重要である。狭窄性病変を有する部にしばしば厚いプラークを伴う瘤状拡張がみられる場合もあり，このような症例においては腹部大動脈瘤などを合併する事も多い。また，内腸骨動脈の分岐や開存の有無，側副路の状態を把握しておく事も重要である。腸骨動脈において内腸骨動脈近傍に病変が存在する場合，内腸骨動脈をまたぐようにステントを挿入せざるを得ない症例も多い。多くの場合，臨床的に問題となることはないが，反対側の内腸骨動脈の開存の有無や腰動脈などの側副路となりうる血管の状態を把握しておくことは重要である。事前の情報収集で最も重要なことはアクセスルートを決めることであるが，我々はできるだけ病変と同側で近い位置からの治療を原則としている。これは治療の難易度を下げ，より安全にかつ短時間に治療を行うために重要なポイントと考える。ただし，総大腿動脈の拍動を触れにくいため，穿刺には慣れも必要である。同側からのアプローチだけでなく，反対側からのアプローチも行い，穿刺の際には反対側から挿入したカテーテルから造影を行って血管の走行を確かめて穿刺する方法も重要であろう。

腸骨動脈の場合にはステント治療の長期成績が良好であるため，ステント挿入になることが多いが，プラーク量が少ない非常に限局した病変の場合にはバルーンPTAだけで十分な場合もある。バルーンのみで治療する際には，前後の対象血管径と同じかやや大きめのバルーンを使用する。原理上，限局解離が起こるが，小さな解離であれば低圧（1～3気圧）で長時間（3～5分）の拡張を行うことで十分に拡張が得られる事も多い。使用するバルーンは好みにも左右されるが，我々はセミ・コンプライアント・バルーンを使用している。セミ・コンプライアント・バルーンの場合は，定格のバルーン径に広がるための圧（nominal pressure）があり，これより加圧すると若干ではあるがバルーン径を大きくすることもできる。ただし，[illegible] pressureとrated burst pressureの[illegible]のはバルーン径の変化量も大きく，[illegible]広げたい場合に有用であるが，しばしば[illegible]ンの両端のほうが大きく拡張し，病変部[illegible]健常部を広げてしまう結果となる事も[illegible]注意が必要である。また，バルーンは[illegible]留置における前拡張や後拡張においても[illegible]ある。遠位塞栓に関連して前拡張には様々な[illegible]論があるが，我々はステント挿入を前提とした[illegible]場合，4～5mm径のバルーンで前拡張を行っている。過拡張は遠位塞栓の危険性を増すため避けるべきだが，ステント挿入時の不完全拡張や後拡張バルーンの挿入困難が生じないようにする目的がある。

腸骨動脈においてステントは重要なデバイスであるが，ステントにはバルーン拡張型ステントと自己拡張型ステントがある。本邦ではバルーン拡張型ステントで血管用デバイスとして認可を受けているものはPalmaz stent（図1A）のみである。Palmaz stentはスリットが入ったステンレスのチューブがバルーンに載せられた形をしており，radial forceが強く，留置時の位置決めを行いやすい特徴がある。しかし，いったん外圧などで潰れると元に戻らないことや，血管を直線的に伸ばすため外圧がかかりやすい場所や屈曲部には使いにくい。挿入時にはステントの脱落を防ぐため，病変部を超えてシースを挿入し，シースの中でステントを進めて病変部まで持ってきた後，シースを引いてステントを露出させるようにする必要がある。シースを挿入できない場合は事前に十分に血管を広げておき，途中でステントが病変に引っかかって脱落しないように注意する必要がある。

自己拡張型ステントはバルーン拡張型ステントと異なり，自己拡張力があるため，外圧による変形に強い特徴がある。ステントの形態により，拡張力や留置時のステント短縮が異なるが，これらの特徴から考えて大きく二つの製品群に分けられると考える。ひとつはWallstent（図1B）でこれは網の目状に金属ワイヤを編んだもので，拡張しながらステントが短縮する特徴を

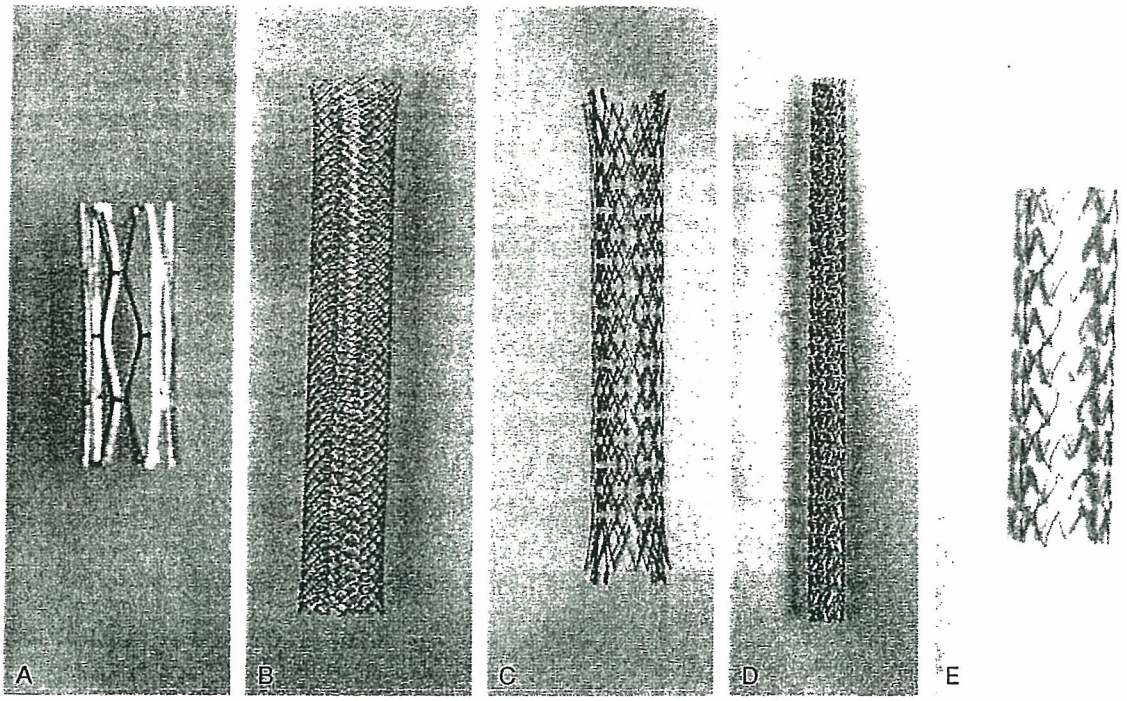

図1　本邦で保険認可されている各種血管用ステント
A　Palmaz stent　唯一のballoon expandable stentである。B　Wallstent　写真はEasy Wallstentである　C　Luminexx
D　SMART er　E　SelfX

持つ。短縮が顕著であるため，ステントの選択や位置決めがややむずかしく，挿入時のテクニック（プッシュ・イン）を要する事もあるがステントメッシュが細かく，ステント内へのプラーク突出をみることが少ないのが特徴である。また，展開途中でもシース内に再収納（リシース）して位置決めをやり直すことができるのも特徴のひとつである。もう一つの製品群はLuminexx（図1C）やSMART stent（図1D）でナイチノールをレーザーカットで形成したものである。留置時の短縮が少なく厳密な留置が可能だが，リシースはできないため，展開前の位置決めと展開時のズレを起こさないような工夫が必要である。これらの最近の製品群にはコントロールハンドルと呼ばれる展開用ツールが手元についており，厳密な位置決めをやりやすくする工夫がみられる。Luminexxでは規格に短いステントがあるのが魅力ではあるが，短いステントを展開しようとする際には，ステントが飛び出して位置がずれないように，あまりゆっくりと展開せずにスピーディに展開するのがコツである。LuminexxとSMART stentの大きな違いはブリッジの本数とstentのオープンエリアの広さにある。Luminexxではステントを長軸方向で接合するブリッジの本数が少ないため，ステント自体の柔軟性を増しているが，ひとつひとつのベンド部分の長さが長いため，各々のベンドのエッジがたってしまうことがある。またオープンエリアも広いため，プラークの内腔突出に注意が必要であるが，内腸骨動脈をまたぐ場合などには血流を阻害することが少ないので優れると思われる。一方，SMARTではブリッジ本数が多いがベンドの長さが短いため，結果としてLuminexxと同等の柔軟性を有しているものと考えられる。また，Luminexxよりもオープンエリアは狭いため，プラークの内腔突出に関しては有利であろう。ただし，Luminexxのデリバリーシステムにみられるチップレス構造はステント留置後のデリバリーシステム抜去時の引っかかりがなく，ステントを誤って移動させてしまう

とがない．また，チップの脱落といった事故が起こらないことは大きな利点である。また，最近SelfX（図1E）が保険認可されたが，これはオープンエリアの小ささはSMARTに近く，ブリッジの本数が少ない点はLuminexxに近い。ただし，各々にデザインは異なるため，屈曲時や伸展時などの特性は異なる。

これらのステントの使い分けは様々な議論があると思われるが，閉塞病変ではプラーク量が多くプラークの内腔突出のリスクも増えると考えられるため，我々はオープンエリアが小さいステントを選択するようにしている。また，病変とは反対側からcross overにアプローチをする際は，短縮が少ないステントを選択する事と，デリバリーシステム抜去時のリスクを減らす事を念頭に置きデバイスを選択したり，また前拡張を行ったりしている。

2）大腿動脈

基本的にはTASC A，Bの病変が適応となると考えられる。また，ステントは大腿動脈では適応外使用となるため，バルーンPTAでの早期再狭窄や急性閉塞のリスクがある場合にのみ使用するのが原則である。ナイチノールステントは開存率を改善させるとの報告がある[9]が，それを基材としたdrug eluting stentでの結果が芳しくないものであったこと[6]を考えるとこの領域におけるステントの使用には現在のところ慎重にならざるを得ない。カッティングバルーンは本邦における代替手段であるが，邦人の血管は細い事も多く，ペリフェラル・カッティングバルーンでは径の不適合となることもある。やはり，基本は低圧・長時間の拡張ということになると考える。

3）膝窩動脈

大腿動脈と基本的に同じだが，屈曲部になるためステントの使用はさらにむずかしくなる。大腿動脈の場合は深大腿動脈が側副路として発達している事も多く，重症化することは少ないが，膝窩動脈の閉塞では側副路の発達が不十分で症状が強い場合も多い。また，外科的処置をするにしても関節部で術後瘢痕による機能障害が起こることもあり，治療が難しい場所でもある。虚血症状が強い場合に限り，我々は治療を行っている。

4）下腿動脈

いわゆる跛行趾ではなく，安静時疼痛や潰瘍を有する症例での救趾目的での治療となる。対象となる血管が細く，閉塞病変が多いため治療が難しい領域でもある。この領域においてsubintimal angioplastyはひとつの選択枝だが，末梢で真腔に抜けているかどうかの判断がつきにくい場合も少なからずある。この場合には超音波断層撮影装置を併用するのが望ましいと思われる。バルーン径はまず3mmを使うようにするが，場合によっては5mmぐらいまでバルーン径を大きくすることもある。正確な対象血管径を測定しにくいのも，この領域の特徴だが，経験的には他部位より過拡張に対し強い印象がある。

❸ 閉塞部の通過に関して

最後に閉塞部の通過に関して記すが，スティフネートや椎骨動脈型などのように先端に少しアングルがついたカテーテルをバックアップとしてガイドワイヤを先行させて，カテーテルを追従させてゆく。ガイドワイヤの選択には術者によって種々の方法があるが，我々は0.035inch親水性コーティーングのガイドワイヤを用い，先端はストレートとアングル型を使い分ける。腸骨動脈の場合，逆行性に通過が困難な場合は順行性アプローチも試みるが，閉塞部内でキャッチングしワイヤを誘導する事もある。腸骨動脈でsubintimal recanalizationの報告もある[17]が，大腿動脈以下と異なり出血性合併症が生じた場合に重症となる可能性が高いと思われ，原則的には血管腔内の再開通を行うべきであろう。

文　献

1）Dormandy JA et al：Management of peripheral arterial disease（PAD）. TASC Working Group. TransAtlantic Inter-Society Consensus（TASC）. J Vasc Surg 31（1 Pt 2）：s1-s296，2000

2）Murphy TP et al：Aortoiliac insufficiency；long term experience with stent placement for treatment. Radiology 231：243-249，2004

3) Galaria II et al：Percutaneous transluminal revascularization for iliac occlusive disease；long-term outcomes in TransAtlantic Inter-Society Consensus A and B lesions. Ann Vasc Surg 19：352-360，2005
4) Uher P et al：Long-term results of stenting for chronic iliac artery occlusion. J Endovasc Ther 9：67-75，2002
5) Balzer JO et al：Percutaneous interventional reconstruction of the iliac arteries；primary and long-term success rate in selected TASC C and D lesions. Eur Radiol 16：124-131，2006
6) Duda SH et al：Sirolimus-eluting versus bare nitinol stent for obstructive superficial femoral artery disease；the SIROCCO II trial. J Vasc Interv Radiol 16：331-338，2005
7) Duda SH et al：Sirolimus-eluting stents for the treatment of obstructive superficial femoral artery disease；six-month results. Circulation 106：1505-1509，2002
8) Laird JR：Limitations of percutaneous transluminal angioplasty and stenting for the treatment of disease of the superficial femoral and popliteal arteries. J Endovasc Ther 13 Suppl 2（II30-40），2006
9) Sabeti S et al：Primary patency of femoropopliteal arteries treated with nitinol versus stainless steel self-expanding stents；propensity score-adjusted analysis. Radiology 232：516-521，2004
10) Bolia A et al：Percutaneous transluminal angioplasty of occlusions of the femoral and popliteal arteries by subintimal dissection. Cardiovasc Intervent Radiol 13：357-363，1990
11) Bolia A et al：Recanalisation of femoro-popliteal occlusions；improving success rate by subintimal recanalisation. Clin Radiol 40：325，1989
12) Atar E et al：Balloon angioplasty of popliteal and crural arteries in elderly with critical chronic limb ischemia. Eur J Radiol 53：287-292，2005
13) Bolia A：Subintimal angioplasty in lower limb ischaemia. J Cardiovasc Surg（Torino）46：385-394，2005
14) Kudo T et al：The effectiveness of percutaneous transluminal angioplasty for the treatment of critical limb ischemia；a 10-year experience. J Vasc Surg 41：423-435；discussion 435，2005
15) Mousa A et al：Percutaneous endovascular treatment for chronic limb ischemia. Ann Vasc Surg 19：186-191，2005
16) Spinosa DJ et al：Percutaneous intentional extraluminal recanalization in patients with chronic critical limb ischemia. Radiology 232：499-507，2004
17) Bolia A et al：Recanalization of iliac artery occlusion by subintimal dissection using the ipsilateral and the contralateral approach. Clin Radiol 52：684-687，1997

Increase in Cell Adhesiveness on a Poly(ethylene terephthalate) Fabric by Sintered Hydroxyapatite Nanocrystal Coating in the Development of an Artificial Blood Vessel

Tsutomu Furuzono,* Miwa Masuda,* Masahiro Okada,* Shoji Yasuda,* Hiroyuki Kadono,*† Ryoichi Tanaka,‡ and Kunio Miyatake§

Nano-scaled sintered hydroxyapatite (HAp) crystals were covalently linked onto a poly(ethylene terephthalate) (PET) fabric substrate chemically modified by graft polymerization with γ-methacryloxypropyl triethoxysilane (MPTS) for development of an artificial blood vessel. The weight gain of graft polymerization with poly(MPTS) on PET in benzyl alcohol containing H_2O_2 as an initiator increased as increasing the reaction time and finally reached a plateau value of about 3.5 wt%. The surface characterization of surface modification with poly(MPTS)-grafting was conducted by x-ray photoelectron spectroscopy. HAp nanocrystals of approximately 50 nm in diameter, monodispersed in pure ethanol, were coupled with alkoxysilyl groups of the poly(MPTS)-grafted PET substrate. The HAp nanocrystals were uniformly and strongly coated on the surface of the PET fabrics, although HAp particles adsorbed physically on the original PET without poly(MPTS) grafting were almost removed by ultrasonic wave treatment. More human umbilical vein endothelial cells adhered to the HAp/PET composite fabric compared with original PET after only 4 hours of initial incubation, and the same was observed on the collagen-coated PET. The coating of sintered HAp nanocrystals imparted bioactivity to the polyester substrate, which is a widely used biomedical polymer, without a coating of adhesion proteins derived from animals, such as collagen or gelatin. A prototype of an artificial blood vessel was finally fabricated by use of HAp/PET composite. *ASAIO Journal* 2006; 52:315–320.

Hydroxyapatite (HAp) has attracted considerable attention as hard-tissue–compatible material for implants and bone augmentation procedures, because it bonds directly to bone when implanted[1–5] and results in the formation of a strong bone-implant interface. In addition, HAp ceramics are compatible with soft tissue such as skin through the development of a percutaneous device.[6] We have developed an inorganic-organic composite consisting of nano-scaled sintered HAp crystals[7–9] and biomedical polymers (such as silk fiber) via covalent bonding at the interface.[10–12] Recently, a novel percutaneous device was developed using that inorganic-organic composite.[13] The actual effectiveness as a percutaneous device was evaluated by animal implant experiment. In these continuous studies, one of the reasons for using silk fiber as a polymer substrate is simply for surface modification because of the large number of functional groups on the polymer surface.

If our HAp nanocrystal coating technique can be applied to other medical polymers as well as silk fiber, the uses are expected to spread widely in medical fields. In this regard, polyester has been used as a typical and popular biomedical polymer, such as in artificial blood vessels[14] and ligaments.[15] Medical devices made of polyester (*e.g.*, artificial blood vessels) are generally coated with collagen or gelatin in order to increase interaction with living cells or tissue. Although the use of animal-derivative proteins is feared due to the possible outbreak of infectious diseases such as bovine spongiform encephalopathy (BSE), the HAp coating is biologically safe because it has no biologic derivative substances.

In this study, we developed a novel composite consisting of nano-scaled HAp crystals and a poly(ethylene terephthalate) (PET) fabric as a polymer substrate through covalent linkage for the purpose of development of an artificial blood vessel. Donation of covalent boding between HAp and the substrate was performed by a coupling reaction between hydroxyl groups on a HAp crystal and alkoxysilyl groups of the graft-polymer on the PET. Surface modification of polyester is relatively more difficult compared with a silk substrate, because functional groups seldom exist on the polyester surface. Hydrophilic moieties were, therefore, introduced on the surface by alkaline hydrolysis as a pretreatment for graft polymerization on PET.

Materials and Methods

Materials

The PET fabric (NBC Inc., Tokyo, Japan) and fiber (1.2 *d*, Teijin Fiber Ltd., Osaka, Japan) selected as typical polyesters were cleaned by soxhlet extraction with methanol for 24 hours, rinsed with distilled water, and dried at 60°C for 24 hours. γ-Methacryloxypropyl triethoxysilane (MPTS) was kindly donated by Shin-Etsu Chemical Co. Ltd. of Tokyo,

From the *Department of Bioengineering, Advanced Medical Engineering Center, National Cardiovascular Center Research Institute, Osaka, Japan; †Institute of Biomaterials and Bioengineering, Tokyo Medical and Dental University, Tokyo, Japan; ‡Department of Radiology, National Cardiovascular Center, Osaka, Japan; and §National Hospital Organization Osaka Minami Medical Center, Osaka, Japan.

Submitted for consideration August 2005; accepted for publication in revised form January 2006.The work was supported by promoting projects on Comprehensive Research on Cardiovascular Diseases

Reprint Requests: Dr. Tsutomu Furuzono, Department of Bioengineering, Advanced Medical Engineering Center, National Cardiovascular Center Research Institute, 5-7-1 Fujishirodai, Suita, Osaka 565-8565, Japan, Tel: +81-6-6833-5012 (ext 2623), Fax: +81-6-6872-7485.

DOI: 10.1097/01.mat.0000214860.08820.f9

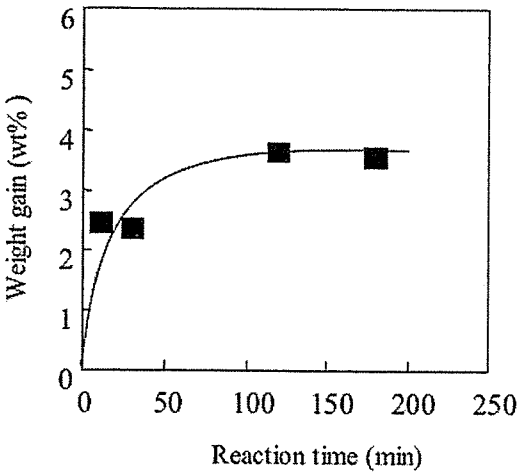

Figure 1. Weight gain of poly(MPTS)-grafted PET as a function of reaction time. Weight gain data were calculated as means of quadruplicate determinations. Error bars represent the standard deviation from the mean, and are included in the closed squares.

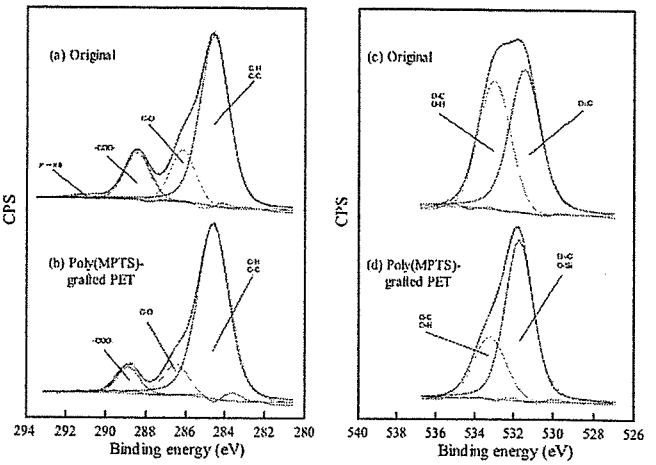

Figure 2. The XPS spectra of (a) original PET and (b) poly(MPTS)-grafted PET.

Japan. Benzyl alcohol (guaranteed reagent; Nacalai Tesque Inc., Kyoto, Japan), methanol (superior quality of reagent; WAKO Pure Chemicals Industries Ltd., Osaka, Japan), and 3% content H_2O_2 (superior quality of reagent; Sigma, Tokyo, Japan) were used without further purification. Water was purified with a Milli-Q system (Millipore Corp., Bedford, MA). HAp crystals with an average diameter of 50 nm were prepared by an alternating emulsion system and subsequently calcinated at 800°C for 1 hour, using a sintering agent such as calcium hydroxide as described in our previous reports.[7–9]

Graft Polymerization

Graft polymerization of MPTS onto alkaline-hydrolyzed PET fabric[16] was conducted using H_2O_2 as an initiator.[17] The PET fabric was carefully immersed in a 0.2 N aqueous NaOH solution for 30 minutes at 60°C and then rinsed with Milli-Q water in order to generate carboxyl groups on the surface. Carboxylate-functionalized PET fabric (0.03 g) was added into a 100-ml flask equipped with an inlet of N_2, a reflux condenser, and a stirrer, and then purged with N_2 for 30 minutes. As an initiator, 40 ml benzyl alcohol containing 785 μl H_2O_2 (100 mEq/l) was added to the flask. Subsequently, 10 ml (50 v/v%) MPTS monomer in benzyl alcohol was added, and the content was stirred occasionally during polymerization for a defined period. After the polymerization, the PET fabric was washed with ethanol several times to stop polymerization in order to remove ungrafted homopolymers formed during polymerization, and then dried under reduced pressure at 1.0 mm Hg for 24 hours at 70°C. The weight gain after polymerization was calculated from the following equation:

$$\text{Weight gain} = (W_2 - W_1)/W_1 \times 100$$

Table 1. Atomic Compositions on PET Surfaces Measured by XPS

Sample	C	O	Si
Original PET (atom%)	69.5	29.5	0.64
Poly(MPTS)-grafted PET (atom%)	60.7	29.5	9.76

where W_1 and W_2 are the weight of the dried original PET and the PET after the polymerization, respectively.

Coating of HAp Nanocrystals on PET

The poly(MPTS)-grafted PET fabric was soaked in the HAp suspension (2.0 wt/v%) in ethanol for 1 hour at room temperature to adsorb the crystals on the grafted PET. The fabric adsorbed with HAp particles was strongly washed by stirring in ethanol, and heated at 80°C for 2 hours under vacuum (1 mm Hg) in order to achieve the reaction between OH groups on the HAp crystals and ethoxysilyl groups on the poly(MPTS)-grafted PET. The composite was washed in ethanol using an ultra sonic generator for 1 minute (output: 20 kHz and 35 W) to remove unreacted HAp particles physically adsorbed on other particles. The composite was finally washed in a large amount of ethanol and pure water for 1 day to remove the residual organic solvents used in polymerization.

Cell Adhesiveness

Human umbilical vein endothelial cells (HUVEC) were incubated in endothelial cell basal medium-2 (EGM-2, supplemented with heat-inactivated 5% FBS, 1 mg/ml gentamicin/amphotericin B) in air containing 5% CO_2 at 37°C. The HUVEC were plated onto the HAp/PET composite fabric in 24-well multiplates at 1×10^5 cells/ml in EGM-2, and incubated at 37°C for 4 hours. After the fabrics adhered to the cells, they were washed twice in phosphate-buffered saline [PBS (–)], fixed with 2.5% buffered glutaraldehyde for 20 minutes at 30°C, and then rinsed with PBS(–) three times. The cells were dehydrated with aqueous ethanol (50–100%) and 100% *n*-butanol for 5 minutes at room temperature step by step. The samples were lyophilized and coated with gold. The morphology of the cells on the samples was observed by scanning electron microscopy (SEM). In the fluorescence observation, the nuclei of HUVEC on the fabric were stained with 1 μM Hoechst 33342 (Wako Pure Chemical Industries Ltd., Tokyo, Japan), and observed by fluorescence microscopy (Eclipse TE300, Nikon Co., Tokyo, Japan). In the cell adhesion experiment, 0.03; collagen-

Table 2. Results of the Peak Separations for C_{1s} and O_{1s} Spectra Measured by XPS

		C_{1s}				O_{1s}	
Binding energy	(eV)	284.6	286.2	288.5	291.0	531.5	533.0
Chemical state		C-H C-C	C-O	-COO-	$\pi \rightarrow \pi^*$	O=C O-Si	O-C O-H
Original PET	(atom%)	67.7	16.2	15.1	1.0	55.4	44.6
Poly(MPTS)-grafted PET	(atom%)	81.5	10.6	7.9	0.0	72.0	28.0

coated (Cellmatrix Type I-C, Nitta Gelatin Inc. Osaka, Japan) PET fabric was used as a positive control.

Measurements

Weight gain was measured by using a high precise balance (GR-202, A&T Co. Ltd., Tokyo, Japan), which shows 0.01 mg of the minimum weight (±0.02 mg). The HAp/PET composite and its cell morphology were observed with a 5 kV scanning electron microscope (SEM; JSM-6301F, JEOL, Tokyo, Japan). To characterize the surface-modified samples, x-ray photoelectron spectroscopy (XPS, 1600S type, PHI Inc., Tokyo, Japan) was used. The power of the nonmonochromated MgKα source was 100 W with an investigated size of 0.8 × 2.0 mm. Tensile properties were measured with the use of a Tensilon RTC-115 OA (Orientic Co. Tokyo, Japan) at an elongation of 50 mm/min. Measurement was conducted with 60 pieces of fiber samples of 40 mm long at 20°C and relative humidity of 65%. Data of weight gain and tensile properties were calculated as means of quadruplicate determinations. Error bars represent standard deviation from the mean. Statistical comparisons were performed with the use of the Student's *t* test, and *p* values less than 0.01 were considered significant.

Results and Discussion

Graft Polymerization

The HAp nanocrystals were covalently coated on the PET fabric through poly(MPTS)-grafted polymers. Alkoxysilyl groups of MPTS can be coupled with OH groups on HAp surfaces. Before coating the HAp crystals, it was necessary to chemically modify the PET surface by radical donation. Many methods of radical donation on a polymer surface are used to graft polymerize with vinyl monomers on PET, such as high-energy radiation of j-rays,[18] benzoyl peroxide,[19] hydrogen peroxide,[20] and persulfate.[21] For graft polymerization of MPTS on PET, we used H_2O_2 in benzyl alcohol as an initiator according to the method of Hebeish *et al.*,[17] because H_2O_2 treatment is easy to handle and a large facility is not necessary. The graft polymerization of MPTS on PET after the radical donation with H_2O_2 could not be accomplished, although the graft polymerization procedure was, at first, faithfully performed. The process of weak hydrolysis of the 0.2 N aqueous NaOH solution used to donate carboxylate functional groups, therefore, was added before the H_2O_2 treatment. **Figure 1** shows the weight gain of poly(MPTS) on the PET fabric, which was plotted as a function of the reaction time. The error bars representing standard deviation of quadruplicates determinations are included in closed squares in the figure. The weight gain of poly(MPTS) increased with increasing reaction time, and eventually reaching a plateau value of about 3.5 wt% using PET fabric consisting of a fiber diameter of 30 μm. However, Hebeish *et al.* reported a of 4.0 wt% maximum weight gain of graft polymerization of polyacrylic acid (AAc) on 1.2-denier PET consisting of a 11 μm fiber diameter in the same reaction solvent.[17] Compared with our simple calculation, the existing monomer ratios of poly(MPTS) and poly(AAc) per a unit of PET surface are 0.9×10^{-3} and 1.4×10^{-3} mol/m^2, respectively. The difference might depend on monomer reactivity for the solvent.

In the characterization of graft polymerization of poly(MPTS) on PET using attenuated total reflection Fourier transform infrared spectrometry (ATR FT-IR), the sign of the grafting with 3.5 wt% was not observed because the band of the Si-O-C stretching vibration of the alkoxysilyl groups overlapped with strong adsorption of an ester (C-O) stretching vibration of the PET substrate at around 1,100 cm^{-1}. Thus, XPS measurement, which enables a more sensitive surface analysis, was performed to characterize the graft surface (3.5 wt%) of PET. **Table 1** shows the change in the atomic proportions on the outermost surface of the original and poly(MPTS)-grafted PET. Although the atomic ratio of the carbon of poly(MPTS)-grafted PET was lower than that of the original PET, the silicon of the grafted PET was higher than that of the original one. The original PET initially contained a very small quantity of silicon contamination. This impurity is assumed to get mixed in during the manufacturing process of PET. **Figure 2** shows XPS C_{1s} and O_{1s} spectra of the original and grafted PET, and **Table 2** shows the quantified data from the area of the curve fitting these XPS signals. With high resolution of XPS C_{1s} spectra, they were resolved at 284.6, 28.62, 288.5, and 291.0 eV due to the C-C/C-H, C-O, -COO-, and $\pi \rightarrow \pi^*$ components, respectively.

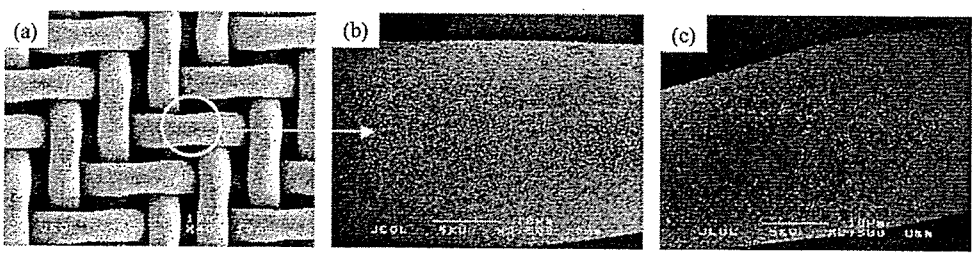

Figure 3. SEM photographs of HAp particles covalently coated on a PET fabric. Lower magnification of HAp/PET composite surface after ultrasonic treatment, (b) higher magnification of HAp/PET composite surface of (a), (c) higher magnification of HAp nanocrystals adsorbed on original PET surface after ultrasonic treatment.

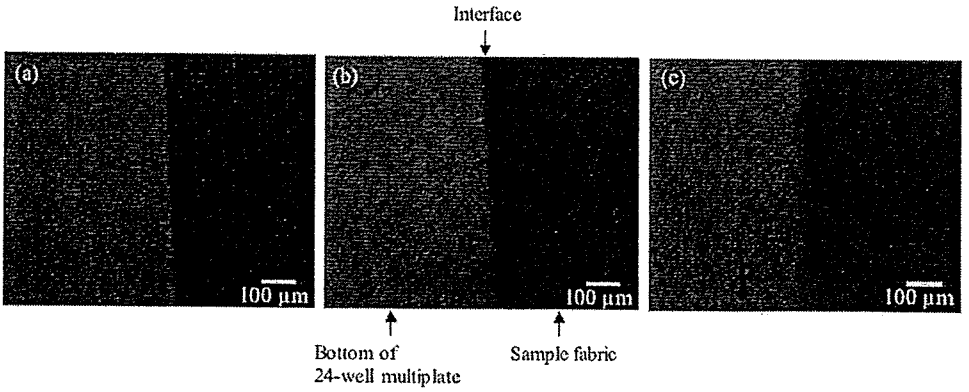

Figure 4. Optical microscopic images of cell toxicity on (a) original PET, (b) poly(MPTS)-grafted PET and (c) HAp/PET composite were incubated after 24 hours.

Although the area of the C-C/C-H component of the grafted PET increased compared with that of the original PET, the area of the C-O and –COO- components decreased. In O_{1s} spectra, however, they were resolved at 531.5 and 533.0 eV due to the O = C(O-Si) and O-C/O-H components, respectively. After graft polymerization of poly(MPTS), the area of O = C(O-Si) and O-C/O-H increased and decreased, respectively. For the control of poly(MPTS)-grafted PET, XPS measurement was conducted against the sample fabric that was adsorbed with MPTS homopolymers and washed strongly with a large amount of ethanol. The value of the silicon component was almost the same as the original PET in the XPS spectra. From the XPS results, it was clear that graft polymerization on PET was well conducted by our process.

Coating of HAp Nanocrystals on PET

The HAp crystals were coated on poly(MPTS)-grafted PET fabric through covalent bonding. Because the covalent bonding could not be observed directly, the chemical bonding was estimated indirectly using a FT-IR analysis that has been described in previous literature.[10] **Figures 3a** and **3b** show SEM photographs of HAp/PET fabric after treatment with an ultrasonic generator. As for the negative control, an SEM image of the original PET surface after ultrasonic treatment on the non-grafted PET surface adsorbed with HAp nanocrystals is shown in **Figure 3c**. Although the HAp crystals adsorbed on the original fabric were almost removed by the ultrasonic treatment, they strongly adhered to the poly(MPTS)-grafted PET surface. The crystals could be uniformly coated with almost every crystal without severe aggregations, because almost all single-dispersed nanocrystals in a medium can be developed using antisintering agents.[9]

For tensile properties measurement, a PET fiber was used because a fabric was very difficult for determination of exact values. Tensile strength and elongation at break were measured with the use of HAp crystal coated 60 pieces of PET fiber by means of quadruplicate determinations. The values of tensile strength of original PET and HAp/PET showed at 468 ± 5 and 417 ± 13 MPa, respectively. The tensile strength of HAp/PET was lower statically by about 10% than that of original PET by using the Student's *t* test. On the other hand, the values of the elongation at break indicated at 24.4 ± 0.8 and 23.0 ± 3.0%, respectively. Although there was no difference statically between the values, it showed a tendency to slightly decrease by HAp coating. In previous studies, HAp coating did not damage the mechanical strength of the substrates, such as silicone sheet[22] and silk fiber.[11] Before HAp coating, in this case, PET was hydrolyzed by 0.2 N aqueous NaOH solution to introduce functional groups on the surface. The alkaline-hydrolysis in the pretreatment process assumes to affect the decrease of mechanical properties. We are now trying new coating process to present no mechanical disadvantage. Actually, the HAp coating PET fabric remained as flexible as the original fabric.

Cell Adhesiveness

To evaluate cell toxicity simply, at first the interface of cells/fabric of the original PET, poly(MPTS)-grafted PET and HAp/PET composite incubated for 2 days were observed by using an optical microscope (**Figure 4**). The sample fabrics were cut in half and put into the bottom of a 24-well multiplate. The cells around the interface of the fabrics of poly(MPTS)-grafted PET and the HAp/PET composite adhered and proliferated well, the same as those on the original PET. Therefore, it was clear that the composite material did not express cell toxicity. **Figures 5** and **6**, respectively, show SEM images of HUVEC morphologies and fluorescence images of stained nuclei of HUVEC on sample substrates after 4 hours of

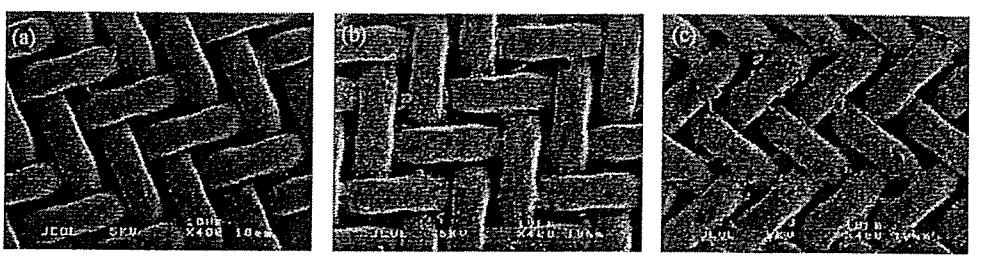

Figure 5. Scanning electron microscopy photographs of HUVEC adhering to (a) original PET, (b) collagen-coated PET, and (c) HAp/PET composite.

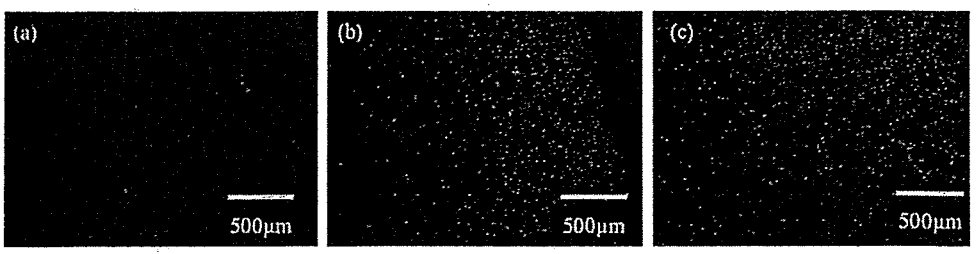

Figure 6. Fluorescence photographs of HUVEC nuclei on (a) original PET fabric, (b) collagen-coated PET, and (c) HAp/PET composite.

incubation. The initial interaction of HUVEC on substrates was evaluated after 4h of incubation, according to several reports.[23,24] In the SEM images, it seemed that many cells adhered on HAp/PET fabric as well as collagen-coated PET, while only a few cells adhered on the original fabric. The difference in the number of cells which adhered could not be distinguished by SEM observation, since HUVEC were flattened and spread over the substrate. The cells which adhered were then stained by fluorescent stain and observed by a fluorescence microscope. It was found that the number of cells which adhered on HAp/PET was qualitatively the same as that of collagen-coated PET, although the cells seldom adhered on the original PET for such a short period of incubation. This phenomenon may be explained by the fact that cell adhesion proteins, such as fibronectin, vitronectin, etc. in FBS of a culture medium, may be favorably adsorbed on the HAp surface.[13] In other words, it is clear that calcinated HAp coating on popular biomedical substrates is effective to obtain the affinity of cells without using biological scaffold proteins such as collagen or gelatin. It can be said that the HAp/PET composite is very meaningful for biological safety in medical fields today when the danger of BSE infection by using proteins derived from a bovine animal is trumpeted loudly. A prototype of artificial blood vessel made of the HAp/PET composite was fabricated (**Figure 7**), and the effect of HAp nanocrystals on it through animal implantation experiments *in vivo* is being evaluated now.

In conclusion, a novel composite consisting of nano-scaled HAp crystals and PET through covalent linkage was developed. In a cell toxicity test, it was confirmed that the HAp/PET composite was nontoxic, and HUVEC adhered more plentifully on the HAp/PET composite compared to the original PET and to the same degree as collagen-coated PET after only 4 hours of incubation. This result demonstrates that the coating of sintered HAp nanocrystals is a simple method for making a polyester substrate bioactive, and that the coating of HAp nanocrystals is superior in the terms of biologic safety.

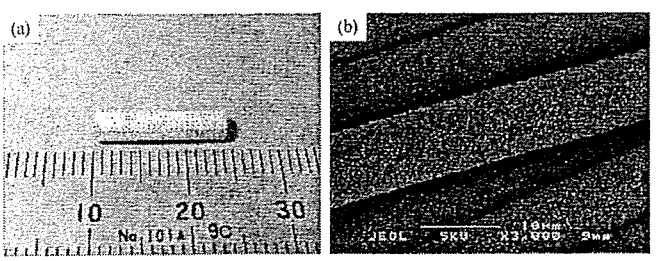

Figure 7. The images show a prototype of an artificial blood vessel made of HAp/PET composite. (a) External view of the prototype. (b) SEM image of HAp/PET fibers inside of the prototype.

References

1. Deligianni DD, Katsala ND, Koutsoukos PG, Missirlis YF: Effect of surface roughness of hydroxyapatite on human bone marrow cell adhesion, proliferation, differentiation and detachment strength. *Biomaterials* 22: 87–96, 2001.
2. De Bruijn JD, Van Blitterswijk CA, Davies JE: Initial bone matrix formation at the hydroxyapatite interface in vivo. *J Biomed Mater Res* 29: 89–99, 1995.
3. Jarcho M: Calcium phosphate ceramics as hard tissue prosthetics. *Clin Orthop* 157: 259–278, 1981.
4. Jarcho M: Retrospective analysis of hydroxyapatite development for oral implant applications. *Dent Clin North Am* 36: 19–26, 1992.
5. Okumura M, Ohgushi H, Dohi Y, *et al*: Osteoblastic phenotype expression on the surface of hydroxyapatite ceramics. *J Biomed Mater Res* 37: 122–129, 1997.
6. AOKI H: *Medical Applications of Hydroxyapatite,* Ishiyaku EuroAmerica Inc., 1994.
7. Furuzono T, Walsh D, Sato K, *et al*: Effect of reaction temperature on the morphology and size of hydroxyapatite nanoparticles in an emulsion system. *J Mater Sci Lett* 20: 111–114, 2001.
8. Sonoda K, Furuzono T, Sato K, *et al*: Influence of emulsion on crystal growth of hydroxyapatite. *Solid State Ionics* 151: 321–327, 2002.
9. Okada M, Furuzono T: Nano-sized ceramic particles of hydroxyapatite calcined with an antisintering agent. *J Nanosci Nanotech,* in press.
10. Furuzono T, Tanaka J, Kishida A: Nano-scaled hydroxyapatite/polymer composite I. Coating of sintered hydroxyapatite particles on poly(gamma-methacryloxypropyl trimethoxysilane-)grafted silk fibroin fibers through chemical bonding. *J Mater Sci Mater Med* 15: 19–23, 2004.
11. Korematsu A, Furuzono T, Yasuda S, *et al*: Nano-scaled hydroxyapatite/polymer composite II. Coating of sintered hydroxyapatite particles on poly(2-(o-[1'-methylpropylideneamino] carboxyamino) ethyl methacrylate)-grafted silk fibroin fibers through covalent linkage. *J Mater Sci* 39: 3221–3225, 2004.
12. Korematsu A, Tsutomu F, Yasuda S, Tanaka J, Kishida: Nano-scaled hydroxyapatite/polymer composite III. Coating of sintered hydroxyapatite particles on poly(4-methacryloyloxyethyl trimellitate anhydride)-grafted silk fibroin fibers. *J Mater Sci Mater Med* 16: 67–71, 2005.
13. Furuzono T, Yasuda S, Kimura T, *et al*: Nano-scaled hydroxyapatite/polymer composite IV. Fabrication and cell adhesion properties of a three-dimensional scaffold made of composite material with a silk fibroin substrate to develop a percutaneous device. *Artif Organs* 7: 137–144, 2004.
14. Marois Y, Chakfe N, Guidoin R: An albumin-coated polyester arterial graft: In vivo assessment of biocompatibility and healing characteristics. *Biomaterials* 17: 3–14, 1996.
15. Lettry S, Roccavilla F, Seedhom B: Abrasion of artificial ligaments: A simulative study. *J Orthop Sci* 5: 481–488, 2000.
16. Roux S, Demoustier-Champagne S: Surface-initiated polymerization from poly(ethylene terephthalate). *J Polym Sci Part A Polym Chem* 41: 1347–1359, 2003.
17. Hebeish A, Shalaby SE, Bayazeed AM: H_2O_2-induced graft polymerization of acrylic acid on poly(ethylene terephthalate) fibers. *J Appl Poly Sci* 26: 3245–3251, 1981.

18. Dasgupta S: Introduction of dyeability to dye-resistant fibers. *Can Text J* 86: 41–47, 1969.
19. Shalaby SE, Bayzeed AM, Hebeish A: Factors affecting polymerization of 2-methyl-5-vinylpyridine in poly(ethylene terephthalate) fibers using benzoyl peroxide as initiator. *J Appl Polym Sci* 22: 1359–1375, 1978.
20. Hebeish A, Shalaby SE, Ei-Shahid MF: Graft polymerization of 2-methyl-5-vinyl pyridine on poly(ethylene terephtalate) fibres using H_2O_2 as initiator. *Angew Makromol Chem* 66: 139–154, 1978.
21. Sakurada I, Sakaguchi Y, Sakai Y: Modification of polyester fibers by graft copolymerization. *Jpn Pat* 7008: 756 1970. Chem Abstr 73, 46562, 1970
22. Furuzono T, Wang PL, Korematsu A, *et al*: Physical and biological evaluations of sintered hydroxyapatite/silicone composite with covalent bonding for a percutanous implant material. *J Biomed Mater Res Part B Appl Biomater* 65: 217–226, 2003.
23. Hamerli P, Weigel T, Groth T, Paul D: Surface properties of and cell adhesion onto allylamine-plasma-coated polyethylenterephtalat membranes. *Biomaterials* 24: 3989–3999, 2003.
24. Massia SP, Hubbell JA: Human endothelial cell interactions with surface-coupled adhesion peptides on a nonadhesive glass substrate and two polymeric biomaterials. *J Biomed Mater Res* 25: 223–242, 1991.

Advances in Science and Technology Vol. 49 (2006) pp. 37-44
online at http://www.scientific.net

Development of Nano-Ceramic Coating on a Substrate through Covalent Linkage and Its Biological Properties

Tsutomu FURUZONO[1, 2a]

[1]Department of Bioengineering, National Cardiovascular Center Research Institute, 5-7-1 Fujishiro-dai, Suita, Osaka, 565-8565, JAPAN

[2]Innovation Plaza Osaka, 3-1-10 Techno-stage, Izumi, Osaka, 594-1144, JAPAN

E-mail:furuzono@ri.ncvc.go.jp

Keywords: hydroxyapatite, coating, covalent bonding, biological property

Abstract. Hydroxyapatite (HAp) has unique properties for biomaterials such as hard-tissue-compatible material for bone and tooth and also soft-tissue-compatible materials for skin tissue. However, the hard and brittle nature of HAp limits spreading many medical devices. Recently, a unique composite of sintered HAp nano-crystals -- ceramics -- covalently coupled to polymer substrates was developed -- *Nano-Ceramic Coating* --. The development was depended on the two original technologies: (1) control of size/morphology of high-dispersed sintered nano-HAp, (2) donation of covalent bonding between nano-HAp and substrates to coat strongly on the surface. The nano-composite material holds not only the mechanical properties of the substrate but also biological properties of the ceramics coated on the surface. In this report, the method of synthesis of high-dispersed nano-HAp, the preparation of the nano-composite, the biological properties with cells or animal tissue, and especially, the development of medical devices, such as percutaneous device or blood vessel and so on, made of the composite will be presented.

Introduction

Hydroxyapatite (HAp: $Ca_{10}(PO_4)_6(OH)_2$) has unique properties for biomaterials such as hard-tissue-compatible material for bone and tooth also soft-tissue-compatible material for skin tissue. From the point of view of tissue-compatible material made up of HAp, The hard and brittle nature of HAp limits spreading over many medical applications. To overcome the defects of ceramics maintaining the nature of HAp, we developed a novel inorganic-organic composite, which calcined HAp nanoparticles

(crystals) [1] coated on polymer substrate by chemical bonding, such as covalent or ionic linkage [2-5]. The significant feature of our fabrication is formation of a nano-scaled ceramic layer on substrate surface without damage to the mechanical properties of the polymer substrate. The technology of nano-ceramic coating can be applying to increase of adhesiveness between hard materials and soft tissue in living body, and developing novel biomaterials which is compatible for soft-tissue, such as percutaneous device, artificial blood vessel, or a scaffold for regenerative medicine, and so on.

The design of the nano-composite consisting of calcined HAp nanoparticles and polymer substrates depends on two key technologies: (I) control of size, morphology and dispersiveness of calcined HAp nanoparticles, (II) fabrication of inorganic-organic composite by chemical bonding between the interface as shown in **Scheme 1**. In this report, the method of synthesis of high-dispersed nano-HAp, the preparation of the nano-composite, the biological properties with cells or animal tissue, and especially, the development of medical devices, such as percutaneous device or blood vessel and so on, made of the composite were presented.

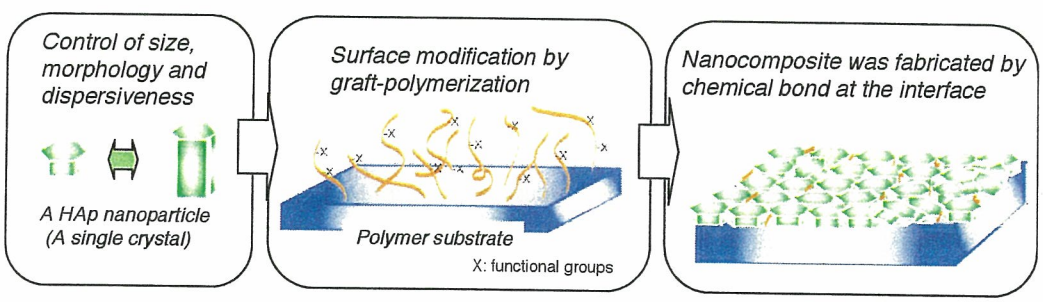

Scheme 1 Schematic presentation of an inorganic-organic composite material by chemical bonding between the interface.

Calcined HAp Nanoparticles for Nanofabrication

This subsection describes the preparation of HAp nanoparticles by calcination with an anti-sintering agent interspersed between the particles and the subsequent removal of the agent [6-8]. There was no contact between the particles during calcination. $Ca(OH)_2$ was selected as an anti-sintering agent because it would not melt at the calcination temperature (800 °C), presumably not dissolve the HAp, and could be removed by washing with water after calcination. The HAp nanoparticles obtained